Dalton Transactions

PAPER

View Article Online
View Journal | View Issue

CrossMark click for updates

Cite this: *Dalton Trans.*, 2017, **46**, 509

Functional polyoxometalates from solvothermal reactions of $VOSO_4$ with tripodal alkoxides – a study on the reactivity of different "tris" derivatives†

Olaf Nachtigall, Adelheid Hagenbach, Jelena Wiecko, Dieter Lentz, Ulrich Abram and Johann Spandl*

Received 19th September 2016,
Accepted 8th December 2016

DOI: 10.1039/c6dt03638d

www.rsc.org/dalton

We report a study on the structure directing effects of functional groups and counterions. The aim was to find a facile and high yielding synthetic procedure to obtain polyoxometalate (POM) building blocks for post-functionalisation. Therefore, solvothermal reactions of $VOSO_4$ with various tris(hydroxymethyl)-methane derivatives in alkaline methanolic solutions were investigated. In doing so, new POM fragments were isolated and characterised. The binding modes of the functionalised tripodal alkoxides turned out to be surprisingly different.

Introduction

Early transition metals like vanadium tend to form anionic metal-oxygen clusters with well-defined structures. A common trend is to introduce heterometals by so-called "capping" to these polyoxometalates (POMs), meaning that some metal ions are replaced by ions of another metal within the metalate structure.[1–7] Thereby, the overall charge of the cluster is often reduced and physical characteristics are altered depending on the added metal. Recent examples are vanadium capped Dawson-type tungstates or molybdates.[1–3] Especially the $[P_2V_3W_{15}O_{62}]^{6-}$ aggregate drew a lot of attention. Therein, three W(VI) ions of the $[P_2W_{18}O_{62}]^{9-}$ are replaced by three V(V) ions. These heterometals form a $[V_3O_{13}]$ fragment within the Dawson-type tungstate and introduce a new reactive side to the polyoxometalate.

Another way to tune the properties of POMs is the functionalisation with organic ligands. An established method is to use 2-(hydroxymethyl)propane-1,3-diol derivatives, which are also referred to as tris(hydroxymethyl)methane (tris) derivatives.[8–13] As depicted in Fig. 1, those tripodal alkoxide ligands are typically found capping tetrahedral voids at the surface of vanadium-based POMs. Thereby, the whole structure is stabilised and the charge of the aggregate is reduced, as oxo groups are replaced by alkoxo groups. By employing such organic ligands, even neutral aggregates may be obtained.

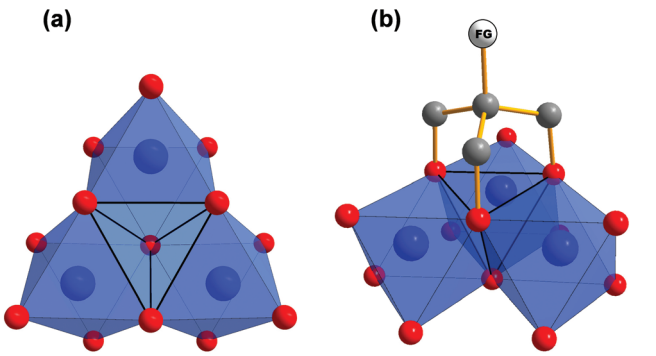

Fig. 1 (a) Polyhedra plot of a $[V_3O_{13}]$ using Diamond software.[38] The tetrahedral void in the centre is highlighted. (b) Tripodal "tris" ligand introducing a functional group (FG) by capping the tetrahedral void. Colour code: vanadium atoms and $[VO_6]$ polyhedra, blue; oxygen atoms, red; carbon atoms, grey.

Our aim was to synthesise versatile building blocks which can be modified by post-functionalisation. Earlier studies showed that interesting coordination complexes, metal–organic frameworks (MOFs), or other hybrid nanoscale systems may be constructed that way.[14–20] To achieve this goal, we have tried to introduce different functionalities at the surface of our POMs by using the functional "tris" derivatives shown in Fig. 2.

The well-known pentaerythrithol (Fig. 2a) is bearing a fourth hydroxymethyl group, which could be useful for silyl or sulfonyl ether formations. The additional bromomethyl group of pentaerythritol monobromide (Fig. 2b) could react with alcoholates in Williamson ether syntheses. More promising are the pyridyl (Fig. 2c) and azido (Fig. 2d) functionalities. The

Freie Universität Berlin, Institut für Chemie und Biochemie, Fabeckstr. 34-36, 14195 Berlin, Germany. E-mail: jspandl@chemie.fu-berlin.de

† Electronic supplementary information (ESI) available. CCDC 1432056–1432062. For ESI and crystallographic data in CIF or other electronic format see DOI: 10.1039/c6dt03638d

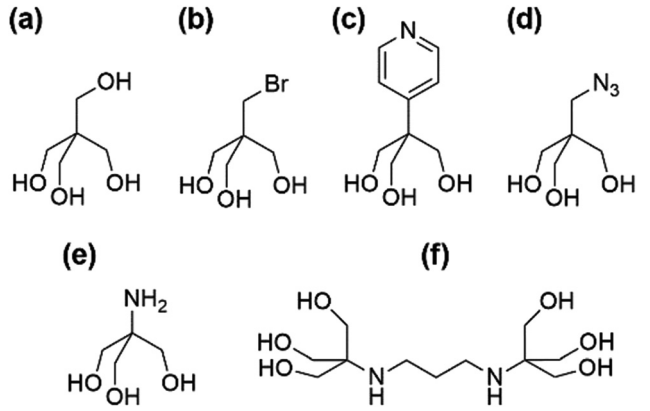

Fig. 2 Functional "tris" derivatives. (a) Tris-CH_2OH (pentaerythritol). (b) Tris-CH_2Br (pentaerythritol monobromide.) (c) Tris-pyridine (2-(hydroxymethyl)-2-(pyridin-4-yl)-propane-1,3-diol). (d) Tris-CH_2N_3 (2-(azidomethyl)-2-(hydroxymethyl)-propane-1,3-diol). (e) Tris-NH_2 ("TRIS", tris(hydroxymethyl)aminomethane). (f) Tris-NH-$(CH_2)_3$-NH-tris (bis–tris propane).

pyridyl group is readily applicable in coordination chemistry while the azido group has a potential synthetic application as 1,3-dipole in cycloadditions like the commonly copper catalysed Huisgen reaction. The most established functional "tris" derivative in POM chemistry is tris(hydroxymethyl)-aminomethane (Fig. 2e) which is often directly referred to as "TRIS". Usually, it is further functionalised by amide couplings before being attached to POMs. Its commercially available dimer "bis–tris propane" (Fig. 2f) is not very valuable for post-functionalisation, but was used for reasons of comparison.

Results and discussion

Functionalised tetranuclear polyoxoalkoxovanadates

Functional groups on tripodal ligands can have a major impact on the POM structure. We found that solvothermal reactions of $VOSO_4$ with tripodal ligands and tetramethylammonium hydroxide in methanol at 125 °C usually yield blue tetranuclear polyoxoalkoxovanadates. Within these planar structures, V(IV) ions are octahedrally coordinated by oxo ligands (Fig. 3a). Four $[VO_6]$ units build a $[V_4O_{16}]$ fragment by being connected *via* common edges (Fig. 3b). This fragment has already been reported for vanadium in oxidation states between +II to +IV.[21,22] Also, such $[V_4]$ aggregates were functionalised with tripodal ligands before.[23,24] This POM structure can be considered as an extract of the well-known decavanadate structure[25,26] or other polyoxovanadates.[27–29] From another perspective, it is an extension of the $[V_3O_{13}]$ fragment by an additional $[VO_6]$ building block.[30–32] Other known $[V_4]$ aggregates are the non-planar butterfly complexes.[33–37]

For our examples, two tripodal ligands are capping the tetrahedral voids on both sides of the aggregates. Bidentate sulfato and methanol ligands are bound to the corners of the POM structure. The different functional groups (R) are pointing away from the vanadium–oxygen framework (Fig. 4a–d). The composition of these ionic compounds was determined to be $[N(CH_3)_4]_2[V_4O_4(CH_3OH)_2(SO_4)_2((OCH_2)_3C\text{-}R)_2]$ (R: $-CH_2OH$ (**I**), $-CH_2Br$ (**II**), $-C_5H_4N$ (**III**), $-CH_2N_3$ (**IV**)).

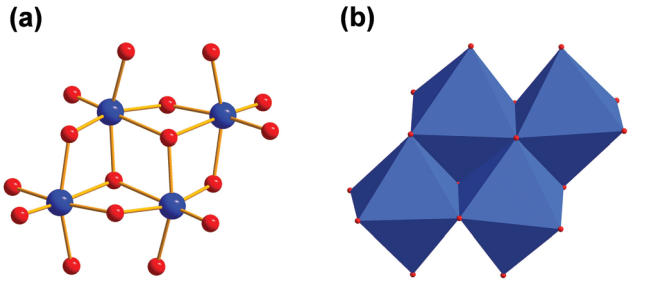

Fig. 3 (a) Vanadium–oxygen framework of $[V_4O_{16}]$ aggregates. (b) Polyhedra plot of $[V_4O_{16}]$ fragment. Colour code: vanadium atoms and $[VO_6]$ polyhedra, blue; oxygen atoms, red.

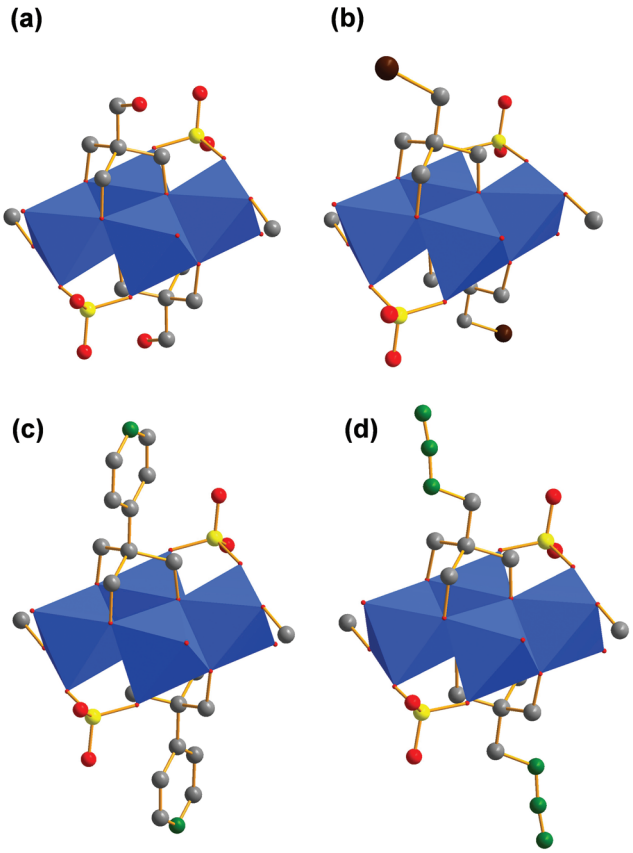

Fig. 4 (a) Polyhedra plot of **I**. (b) Polyhedra plot of **II**. (c) Polyhedra plot of **III**. (d) Polyhedra plot of **IV**. Colour code: vanadium atoms and $[VO_6]$ polyhedra, blue; oxygen atoms, red; carbon atoms, grey; sulphur atoms, yellow; bromine atoms, brown; nitrogen atoms, green.

Hexanuclear polyoxoalkoxovanadate

If the tripodal ligand with a functional amino group (tris-NH_2) is heated with $VOSO_4$ and tetramethylammonium hydroxide in methanol under solvothermal conditions at 125 °C, the grey

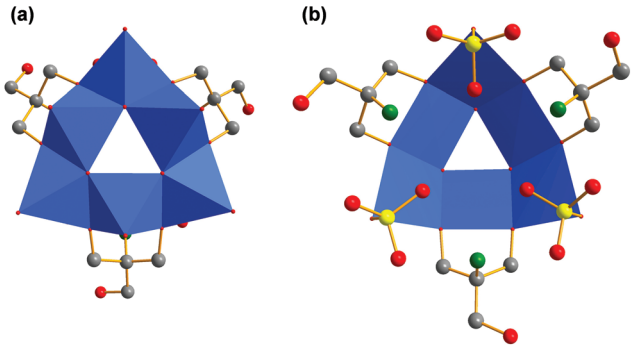

Fig. 5 (a) Polyhedra plot of **V** from the outside of the bowl. (b) Polyhedra plot of **V** from the inside of the bowl. Colour code: vanadium atoms and [VO_6] polyhedra, blue; oxygen atoms, red; carbon atoms, grey; sulphur atoms, yellow; nitrogen atoms, green.

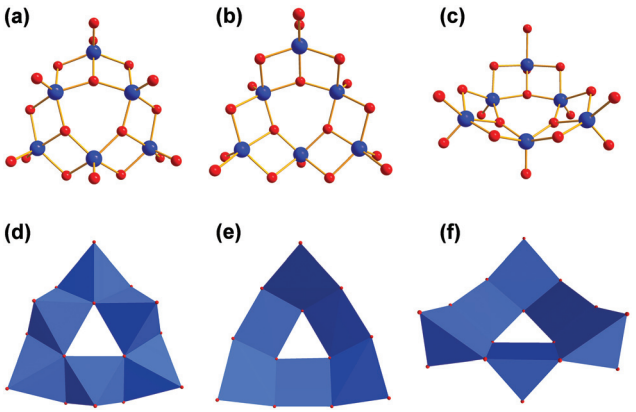

Fig. 6 (a–c) Vanadium–oxygen framework of [V_6O_{18}] aggregate from different perspectives. (d–f) Polyhedra plot of [V_6O_{18}] aggregate from different perspectives. Colour code: vanadium atoms and [VO_6] polyhedra, blue; oxygen atoms, red.

compound $[N(CH_3)_4]_3[V_6O_9(SO_4)_3((OCH_2)_2(HOCH_2)C\text{-}NH_3)_3]$ (**V**) is produced (Fig. 5). The colour change from blue to grey can be assigned to the different coordination sphere of vanadium. Inside the ionic compound **V**, the V(IV) ions are coordinated by oxo ligands in a square pyramidal manner (Fig. 6). The six [VO_5] units are connected *via* common edges in a circular fashion. The overall structure of the [V_6O_{18}] fragment looks like a triangle with a triangular hole in the middle.

Additionally, the structure is not planar but bowl-shaped (Fig. 6c). Three of these fragments associated would give the renown [$V_{18}O_{42}$] cage (Fig. 7).[39,40] Two of the [V_6O_{18}] triangulars linked by boron were reported as well.[41] The same [M_6O_{18}] motif is also known for other metals as part of larger architectures.[42–45] Nevertheless, the single bowl-shaped [V_6O_{18}] fragment has not been published so far. There are other examples of similar [V_5] or [V_9] bowls.[46,47]

Another difference to compounds **I–IV** is the fact that the organic ligands are only binding in a bipodal fashion (Fig. 5b). They bridge three vanadium atoms by sitting on the edges of the triangle. One hydroxymethyl group of each tris-NH_2 protrudes unbound. The protonated amino groups are pointing to the middle of the bowl. As shown in Fig. 5b, they form hydrogen bonds to the sulfato groups of about 2.9 Å (N–O distance). The sulfato ligands bind only in a monodentate way to the vanadium ions at the corners of the triangular fragment. Methanol is not incorporated into the structure. The total charge of the fragment is −3.

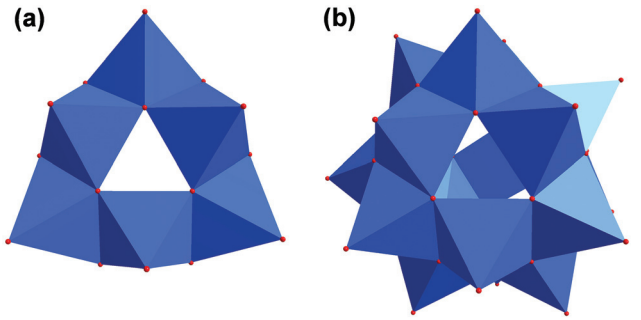

Fig. 7 (a) Polyhedra plot of [V_6O_{18}] aggregate. (b) Polyhedra plot of [$V_{18}O_{42}$] aggregate. Colour code: vanadium atoms and [VO_6] polyhedra, blue; oxygen atoms, red.

Mixed valence heptanuclear polyoxoalkoxovanadate

In avoidance of the structural impact of the free amino group of tris-NH_2, we directly utilised its cross-linked dimer bis–tris propane (tris-NH-$(CH_2)_3$-NH-tris) for the reaction with $VOSO_4$. Instead of getting chains of interlinked [V_4] aggregates, the violet compound $[N(CH_3)_4]_4[V_7O_{11}(CH_3O)(SO_4)_3((OCH_2)_2\text{-}(HOCH_2)C\text{-}NH\text{-}(CH_2)_3\text{-}NH\text{-}C(CH_2OH)(CH_2O)_2)]$ (**VI**) of a discrete size was obtained (Fig. 8). Its [$V_7O_{21}N_2$] framework, shown in Fig. 9a, comprises a square pyramidally all-oxo coordinated V(V) ion and six V(IV) ions (Fig. 9b). Three V(IV) ions have a square pyramidal coordination sphere and are bridged *via* two bidentate sulfato groups at their outer corners (Fig. 8a). They are connected to the V(V) *via* common edges (Fig. 10c and d). The remaining three V(IV) atoms are coordinated octahedrally and from a [V_3] fragment (Fig. 10a and b).[6]

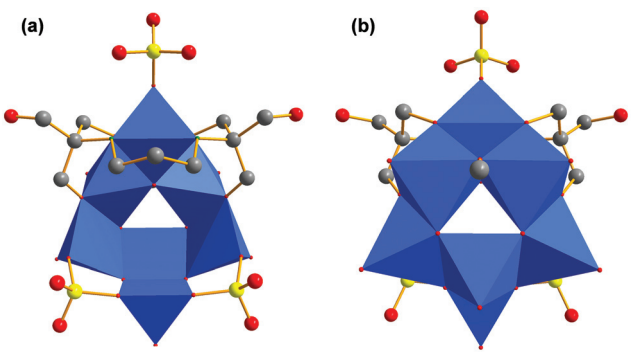

Fig. 8 (a) Polyhedra plot of **VI** from the outside of the bowl. (b) Polyhedra plot of **VI** from the inside of the bowl. Colour code: vanadium atoms and [VO_6] polyhedra, blue; oxygen atoms, red; carbon atoms, grey; sulphur atoms, yellow; nitrogen atoms, green.

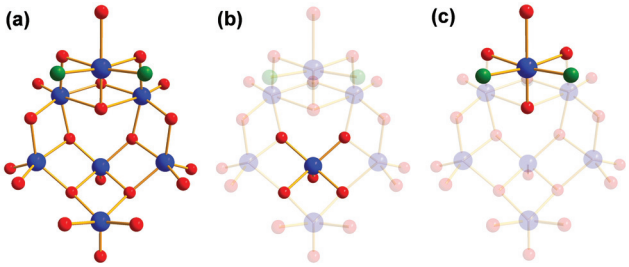

Fig. 9 (a) Vanadium–oxygen–nitrogen framework of $[V_7O_{21}N_2]$ aggregate. (b) Square pyramidally coordinated vanadium (V) ion. (c) Vanadium (IV) ion octahedrally coordinated by four oxygen and two nitrogen atoms. Colour code: vanadium atoms, blue; oxygen atoms, red; nitrogen atoms, green.

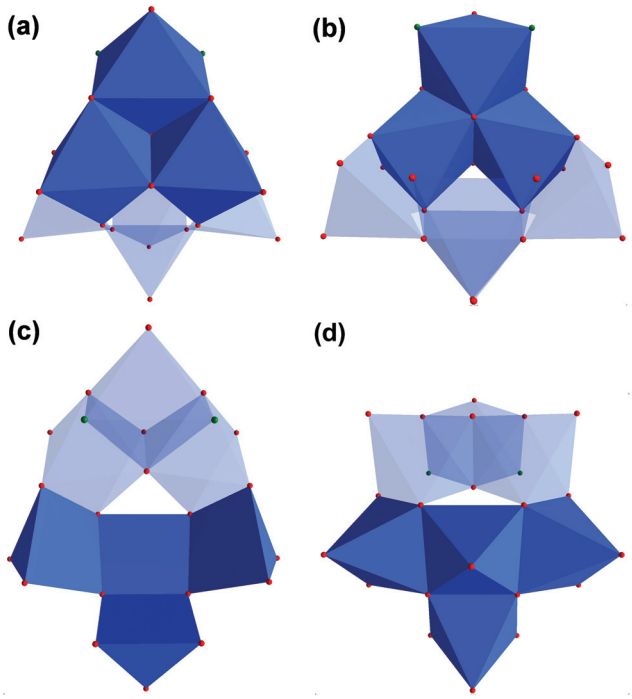

Fig. 10 Polyhedra plots of $[V_7O_{21}N_2]$ fragment. (a) Polyhedra plot of octahedrally coordinated vanadium ions form the outside of the bowl. (b) Polyhedra plot of octahedrally coordinated vanadium ions form the inside of the bowl. (c) Polyhedra plot of square pyramidally coordinated vanadium ions form the inside of the bowl. (d) Polyhedra plot of square pyramidally coordinated vanadium ions form the outside of the bowl. Colour code: $[VO_6]$ polyhedra, blue; oxygen atoms, red; nitrogen atoms, green.

Interestingly, the upper V(IV) ion is coordinated by four oxygen and two nitrogen atoms (Fig. 9c). There are few similar examples.[48] All seven vanadium atoms form a new fragment. Like in substance **V**, the fragment is a bowl-shaped triangle with a triangular hole in the middle. The bis–tris propane ligand entangles the $[V_3]$ motif (Fig. 8a). It binds on each side *via* two hydroxymethyl and the secondary amino group. Again, hydroxymethyl groups protrude unbound. While two bidentate sulfato ligands are linked to the outer square pyramidally

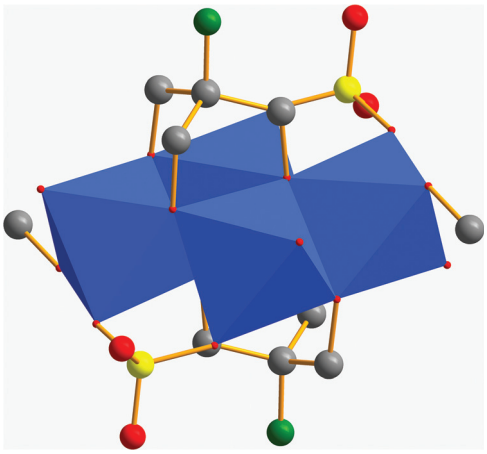

Fig. 11 Polyhedra plot of **VII**. Colour code: $[VO_6]$ polyhedra, blue; oxygen atoms, red; carbon atoms, grey; sulphur atoms, yellow; nitrogen atoms, green.

coordinated V(IV) ions, one monodentate sulfato ligand is bound to the outer octahedrally coordinated V(IV) ion (Fig. 8a). The inner V(IV) ions with an octahedral coordination sphere are bridged by a μ-methoxo ligand (Fig. 8b).

Amino functionalised tetranuclear polyoxoalkoxovanadate

The reactions with other tris derivatives showed that a $[V_4]$ aggregate should be producible with tris-NH_2. Hence, we tried to alter the reaction conditions slightly and varied the counterions. Besides other effects, the counterions influence the solubility of intermediates, byproducts, and products. This intervention in the highly complex equilibrium of possible side reactions can lead to different products. We set up series of reactions with equivalent concentrations of either LiOH, NaOH, KOH, RbOH, or CsOH. The reactions with LiOH, NaOH, RbOH, and CsOH gave amorphous insoluble products. Finally, we succeeded to synthesise an amino-functionalised $[V_4]$ building block by replacing $N(CH_3)_4OH$ by an equivalent concentration of KOH. Instead of an ionic species like **I–IV**, the neutral aggregate $[V_4O_4(CH_3OH)_2(SO_4)_2((OCH_2)_3C\text{-}NH_3)_2]$ (**VII**) was formed (Fig. 11). The two counterions are replaced by the protonation of the two functional amino groups.

Comparison of different binding modes of tris-NH_2

The results show that amino functionalised "tris" ligands can bind in various binding modes (Fig. 12). Tris-NH_2 usually binds in a tripodal fashion capping tetrahedral voids on vanadium POMs with its oxygen atoms (Fig. 12a and b).[17,49] In that way, either three or four vanadium ions are connected like in compound **VII**. This binding mode is found in most publications and is common for the majority of tris derivatives.[8–13]

However, it turned out that tris-NH_2 sometimes reacts differently than other ordinary tris derivatives like tris-CH_3, tris-C_2H_5, or tris-CH_2OH. That is the reason why tris-NH_2 is often functionalised by amide couplings, alkylation, or pro-

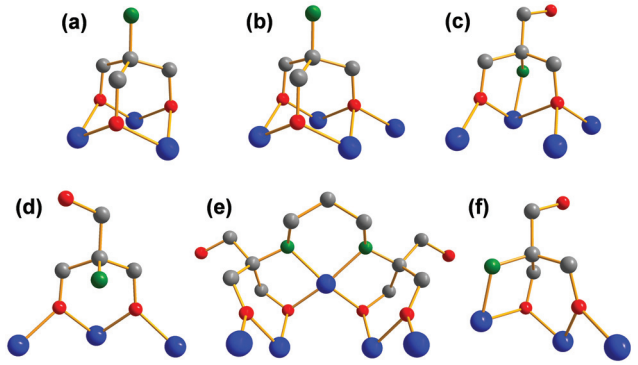

Fig. 12 Different binding modes of tris(hydroxymethyl)-aminomethane ("tris-NH_2 or "TRIS"). (a) Tris-NH_2 connecting three vanadium ions with its three hydroxymethyl groups. (b) Tris-NH_2 connecting four vanadium ions with its three hydroxymethyl groups. (c) Tris-NH_2 connecting four vanadium ions with two hydroxymethyl groups and its amino group. (d) Tris-NH_2 connecting three vanadium ions with two of its hydroxymethyl groups. (e) Dimer of tris-NH_2 ("bis–tris propane") connecting five vanadium ions with four of its six hydroxymethyl groups and its two secondary amino groups. (f) Section of {e} focusing on the binding mode of a single tris-NH moiety within its dimer. The tris-NH moiety is connecting three vanadium ions with two hydroxymethyl groups and its amino group. Colour code: vanadium atoms, blue; oxygen atoms, red; nitrogen atoms, green; carbon atoms, grey.

tected with aldehydes before being reacted with vanadium sources.[20,50,51]

The complex reactivity of free tris-NH_2 with vanadium is insufficiently investigated. Until now, there is only one more tripodal binding mode reported.[52–54] As depicted in Fig. 12c, the amino group can be attached to the vanadium-based POM instead of one of the three alkoxo groups (Fig. 12c). The geometry of the bridged vanadium ions remains the same as in the common binding mode, but the tetrahedral void is not capped by the ligand. In both binding modes, vanadium is coordinated octahedrally.

We found two new binding modes of tris-NH_2 which lead to unexpected vanadium structures. Fig. 12d shows that the ligand can also bind in a bipodal fashion with just two of the three alkoxo groups to vanadates. Thereby, three vanadium ions are connected, but in a more linear than triangular fashion. The coordination sphere of vanadium changes to a square pyramidal arrangement. Like in other known examples, the amino group is protonated.[17]

A second curious binding mode was found when we used "bis–tris propane" (tris-NH-$(CH_2)_3$-NH-tris), the commercially available dimer of tris-NH_2 (Fig. 12e). We highlighted the binding mode of a single tris-NH moiety in Fig. 12f. It shows a third tripodal binding mode. Again, two of the three alkoxo groups are bridging three vanadium ions. In contrast to Fig. 12c, the amino group is attached to one of the outer vanadium ions. Interestingly, the outer vanadium ion that is not directly connected to the amino group is square pyramidally coordinated while the other two vanadium centres possess an octahedral coordination sphere.

Conclusions

In summary, we have shown the structure directing role of functional groups and counterions on our polyoxoalkoxovanadates. By using inexpensive $VOSO_4$ as vanadium source, interesting POM structures were obtained under solvothermal conditions. The results indicate, that functional amino groups have a major impact on our POM structures while hydroxyl, bromo, pyridyl, and azide groups are tolerated. Both primary and even secondary amines can be incorporated within the metal–oxygen framework. This leads to a competition between amino and hydroxyl groups. Hence, the common tripodal binding mode of tris(hydroxymethyl)methane derivatives is challenged if amino groups are incorporated.

Experimental

All compounds could be stored under argon atmosphere at room temperature, but hydrolysed slowly when being exposed to air. The structural analysis was performed on single crystals by X-ray crystallography. The unity of the batches was confirmed by the determination of the unit cells of various crystals. In addition, the crystalline and amorphous parts of the solid products were compared by IR spectroscopy and elemental analysis. The oxidation states of vanadium were calculated by valence sum analysis.[55] All results were in good agreement. The results of the valence sum calulations, an overview of the crystallographic details, as well as the IR spectra with an assignment of the characteristic vibration modes of all compounds are supplied in the ESI.†

Synthetic procedures

All commercially available compounds were used as received without further purification. Elemental compositions were determined on an ELEMENTAR vario EL III. Infrared measurements were performed on a Thermo-Nicolet Nexus 670 FTIR spectrometer with DuraSamplIR accessory in total reflection at room temperature. The IR spectra of all compounds and a table with selected characteristic vibrational frequencies for compounds **I–VII** are supplied in the ESI.†

Tripodal ligands for compounds **III** (tris-pyridine)[56,57] and **IV** (tris-CH_2N_3)[58] were synthesised according to literature.

$[N(CH_3)_4]_2[V_4O_4(CH_3OH)_2(SO_4)_2((OCH_2)_3C\text{-}CH_2OH)_2]$ (I). A 1.4 M solution of tetamethylammonium hydroxide in methanol (0.3 mL, 0.42 mmol) was added to $VOSO_4{\cdot}5H_2O$ (210 mg, 0.83 mmol) and pentaerythritol (tris-CH_2OH) (57 mg, 0.42 mmol) dissolved in methanol (25 mL). The mixture was heated in a sealed Teflon vessel (50 mL) at 125 °C for 24 hours and allowed to cool down slowly to room temperature. **I** was obtained as blue crystalline solid (180 mg, 92%) in a green solution. C, H, N, S (%) = 25.65, 5.55, 2.88, 6.44 (calc. 25.60, 5.37, 2.99, 6.82 for $V_4O_{22}C_{20}H_{50}N_2S_2$). IR ($cm^{-1}$): 3450 (w, br), 1110(m), 1032(m), 1002(s), 959(vs), 947(vs), 622(m), 604(m), 544(vs).

$[N(CH_3)_4]_2[V_4O_4(CH_3OH)_2(SO_4)_2((OCH_2)_3C\text{-}CH_2Br)_2]$ (II). A 1.4 M solution of tetamethylammonium hydroxide in methanol (0.3 mL, 0.42 mmol) was added to $VOSO_4{\cdot}5H_2O$ (210 mg, 0.83 mmol) and 2-(bromomethyl)-2-(hydroxymethyl)-propane-1,3-diol (pentaerythritol monobromide, tris-CH_2Br) (83 mg, 0.42 mmol) dissolved in methanol (25 mL). The mixture was heated in a sealed Teflon vessel (50 mL) at 125 °C for 24 hours. Subsequently, the green solution was reduced to approx. 10 mL under vacuo and stored at −30 °C overnight. **II** was obtained as blue crystalline solid (90 mg, 40%) in a green solution. C, H, N, S (%) = 22.05, 4.74, 2.51, 5.89 (calc. 22.57, 4.55, 2.63, 6.03 for $V_4O_{20}C_{20}H_{48}N_2S_2Br_2$). IR ($cm^{-1}$): 1120(m, sh), 1106(m), 1034(m), 1001(m), 990(m, sh), 957(vs), 944(vs), 659(s), 622(m), 615(m), 544(vs).

$[N(CH_3)_4]_2[V_4O_4(CH_3OH)_2(SO_4)_2((OCH_2)_3C\text{-}C_5H_4N)_2]$ (III). A 1.4 M solution of tetamethylammonium hydroxide in methanol (0.3 mL, 0.42 mmol) was added to $VOSO_4{\cdot}5H_2O$ (210 mg, 0.83 mmol) and 2-(hydroxymethyl)-2-(pyridin-4-yl)-propane-1,3-diol (tris-pyridine) (76 mg, 0.42 mmol) dissolved in methanol (25 mL). The mixture was heated in a sealed Teflon vessel (50 mL) at 125 °C for 24 hours and allowed to cool down slowly to room temperature. **III** was obtained as blue crystalline solid (150 mg, 73%) in a green solution. C, H, N, S (%) = 32.13, 5.09, 5.30, 5.99 (calc. 32.57, 5.08, 5.43, 6.21 for $V_4O_{20}C_{28}H_{52}N_4S_2$). IR ($cm^{-1}$): 1122(m), 1026(m), 1002(m), 956(vs) 939(vs), 609(m), 546(vs).

$[N(CH_3)_4]_2[V_4O_4(CH_3OH)_2(SO_4)_2((OCH_2)_3C\text{-}CH_2N_3)_2]$ (IV). A 1.4 M solution of tetamethylammonium hydroxide in methanol (0.3 mL, 0.42 mmol) was added to $VOSO_4{\cdot}5H_2O$ (210 mg, 0.83 mmol) and 2-(azidomethyl)-2-(hydroxymethyl)-propane-1,3-diol (tris-CH_2N_3) (83 mg, 0.42 mmol) dissolved in methanol (25 mL). The mixture was heated in a sealed Teflon vessel (50 mL) at 125 °C for 24 hours. Subsequently, the green solution was reduced to approx. 10 mL under vacuo and stored at −30 °C overnight. **IV** was obtained as green crystalline solid (55 mg, 45%) in a green solution. C, H, N, S (%) = 24.71, 5.12, 11.66, 6.71 (calc. 24.30, 4.89, 11.34, 6.49 for $V_4O_{20}C_{20}H_{48}N_8S_2$). IR ($cm^{-1}$): 2099(s), 2080(s, sh), 1121(m), 1106(m), 1029(m), 1005(m), 968(vs), 944(vs), 610(m, sh), 546(vs).

$[N(CH_3)_4]_3[V_6O_9(SO_4)_3((OCH_2)_2(HOCH_2)C\text{-}NH_3)_3]$ (V). A 1.4 M solution of tetamethylammonium hydroxide in methanol (0.3 mL, 0.42 mmol) was added to $VOSO_4{\cdot}5H_2O$ (210 mg, 0.83 mmol) and 2-amino-2-(hydroxymethyl)-propane-1,3-diol (tris-NH_2) (51 mg, 0.42 mmol) dissolved in methanol (25 mL). The mixture was heated in a sealed Teflon vessel (50 mL) at 125 °C for 24 hours and allowed to cool down slowly to room temperature. **V** was obtained as grey crystalline solid (150 mg, 82%) in a green solution. C, H, N, S (%) = 21.29, 5.01, 6.20, 7.12 (calc. 21.83, 5.04, 6.36, 7.27 for $V_6O_{30}C_{24}H_{66}N_6S_3$). IR ($cm^{-1}$): 3350(w, br), 1584 (w), 1119(m), 1032(s), 991(s), 976(vs), 945(vs), 722(s), 600 (vs, br).

$[N(CH_3)_4]_4[V_7O_{11}(CH_3O)(SO_4)_3((OCH_2)_2(HOCH_2)C\text{-}NH\text{-}(CH_2)_3\text{-}NH\text{-}C(CH_2OH)(CH_2O)_2)]$ (VI). A 1.4 M solution of tetamethylammonium hydroxide in methanol (0.3 mL, 0.42 mmol) was added to $VOSO_4{\cdot}5H_2O$ (210 mg, 0.83 mmol) and 1,3-bis(tris(hydroxymethyl)methylamino)propane (bis–tris-propane) (59 mg, 0.21 mmol) dissolved in methanol (25 mL). The mixture was heated in a sealed Teflon vessel (50 mL) at 125 °C for 24 hours and allowed to cool down slowly to room temperature. **VI** was obtained as violet crystalline solid (160 mg, 86%) in a green solution. C, H, N, S (%) = 22.78, 5.23, 5.28, 6.36 (calc. 23.57, 5.16, 5.89, 6.74 for $V_7O_{30}C_{28}H_{73}N_6S_3$). IR ($cm^{-1}$): 3450(w, br), 1110(m), 1021(vs), 1000(s, sh), 965(vs), 949 (vs), 708(m), 600(s, br).

$[V_4O_4(CH_3OH)_2(SO_4)_2((OCH_2)_3C\text{-}NH_3)_2]$ (VII). Freshly ground potassium hydroxide (24 mg, 0.42 mmol) was added to a solution of $VOSO_4{\cdot}5H_2O$ (210 mg, 0.83 mmol) and 2-amino-2-(hydroxymethyl)-propane-1,3-diol (tris-NH_2) (51 mg, 0.42 mmol) in methanol (25 mL). The mixture was heated in a sealed Teflon vessel (50 mL) at 125 °C for 24 hours and allowed to cool down slowly to room temperature. **VII** was obtained as blue crystalline solid (130 mg, 80%) in a green solution. C, H, N, S (%) = 15.71, 3.89, 3.25, 7.97 (calc. 15.76, 3.44, 3.68, 8.41 for $V_4O_{20}C_{10}H_{26}N_2S_2$). IR ($cm^{-1}$): 3500(w, br), 1546(w), 1120(m), 1098(s), 1031(m), 996(m), 967(vs), 949(vs), 608(m), 543(vs).

X-ray crystallography

Single crystals of **I**, **III**, **V**, **VI**, and **VII** were directly obtained after cooling the reaction mixtures to room temperature in the Teflon vessel. Since **II** and **IV** are very well soluble in methanol, the volume of the mother liquers had to be reduced under reduced pressure. Subsequent cooling in the freezer at −30 °C yielded crystals of **II** and **IV**. However, the crystal quality of **II**, **V**, and **VI** was rather poor. Recrystallisation of **II** from various solvents did not yield better crystals. Compounds **V** and **VI** are insoluble in allmost all organic solvents and decompose in water. Hence, recrystallisation of **V** and **VI** was not possible. The crystallisation of **VI** from the reaction mixture was improofed by an glassware inlay within the Teflon vessel.

The intensities for the X-ray determinations for **I**, **II**, and **III** were collected on a STOE IPDS 2T instrument. The crystallographic experiments for compounds **IV**, **V**, **VI**, and **VII** were performed on a Bruker X8 Kappa APEX II diffractometer with a CCD-based detector. Mo K_α radiation (λ = 0.71073 Å) was used in all experiments, but for compound **V**. The crystal structure of **V** was determined using Cu radition (λ = 1.54178 Å). Standard procedures were applied for data reduction and absorption correction. All structures were solved by intrinsic or direct methods and refined by full-matrix least-squares on F^2 using the SHELXTL and WinGX programme packages.[59,60] Disordered water molecules in the crystal structures of **II**, **IV**, **V**, and **VI** were treated with PLATON SQUEEZE software.[61] A twin matrix for compound **II** was determined with TwinRotMat.[62]

Crystallographic data for all structures in this publication have been deposited with the Cambridge Crystallographic Data Centre, CCDC 1432056–1432062 (**I–VII**), 12 Union Road, Cambridge CB21EZ, UK.

Acknowledgements

O. N. thanks the Stiftung der Deutschen Wirtschaft for a scholarship.

References

1 H. N. Miras, D. Stone, D.-L. Long, E. J. L. McInnes, P. Kögerler and L. Cronin, *Inorg. Chem.*, 2011, **50**, 8384–8391.
2 H. N. Miras, M. Sorus, J. Hawkett, D. O. Sells, E. J. L. McInnes and L. Cronin, *J. Am. Chem. Soc.*, 2012, **134**, 6980–6983.
3 P. Yin, T. Li, R. S. Forgan, C. Lydon, X. Zuo, Z. N. Zheng, B. Lee, D. Long, L. Cronin and T. Liu, *J. Am. Chem. Soc.*, 2013, **135**, 13425–13432.
4 Y.-B. Liu, L.-W. Fu, W.-J. Duan, L.-N. Xiao, Y.-Y. Hu, D.-C. Zhao, H.-Y. Guo, X.-B. Cui and J.-Q. Xu, *Inorg. Chem. Commun.*, 2014, **47**, 5–8.
5 J. Tucher, S. Schlicht, F. Kollhoff and C. Streb, *Dalton Trans.*, 2014, **43**, 17029–17033.
6 Z. Shi, Y. Zhou, L. Zhang, C. Mu, H. Ren, D. u. Hassan, D. Yang and H. M. Asif, *RSC Adv.*, 2014, **4**, 50277–50284.
7 J.-H. Son and W. H. Casey, *Chem. Commun.*, 2015, **51**, 1436–1438.
8 Q. Chen, D. P. Goshorn, C. P. Scholes, X.-L. Tan and J. Zubieta, *J. Am. Chem. Soc.*, 1992, **114**, 4667–4681.
9 M. I. Khan, Q. Chen, D. P. Goshorn and J. Zubieta, *Inorg. Chem.*, 1993, **32**, 672–680.
10 M. I. Khan, Q. Chen, H. Höpe, S. Parkin, C. J. O'Connor and J. Zubieta, *Inorg. Chem.*, 1993, **32**, 2929–2937.
11 M. I. Khan, Y.-S. Lee, C. J. O'Connor and J. Zubieta, *J. Am. Chem. Soc.*, 1994, **116**, 5001–5002.
12 L. J. Batchelor, R. Shaw, S. J. Markey, M. Helliwell and E. J. L. McInnes, *Chem. – Eur. J.*, 2010, **16**, 5554–5557.
13 L. J. Batchelor, E. Fitzgerald, J. Wolowska, J. J. W. McDouall and E. J. L. McInnes, *Chem. – Eur. J.*, 2010, **16**, 11082–11088.
14 P. R. Marcoux, B. Hasenknopf, J. Vaissermann and P. Gouzerh, *Eur. J. Inorg. Chem.*, 2003, 2406–2412.
15 Y. Q. Hou and C. L. Hill, *J. Am. Chem. Soc.*, 1993, **115**, 11823–11830.
16 J. W. Han, K. I. Hardcastle and C. L. Hill, *Eur. J. Inorg. Chem.*, 2006, 2598–2603.
17 D. Li, J. Song, P. C. Yin, S. Simotwo, A. J. Bassler, Y. Y. Aung, J. E. Roberts, K. I. Hardcastle, C. L. Hill and T. B. Liu, *J. Am. Chem. Soc.*, 2011, **133**, 14010–14016.
18 P. C. Yin, P. F. Wu, Z. C. Xiao, D. Li, E. Bitterlich, J. Zhang, P. Cheng, D. V. Vezenov, T. B. Liu and Y. G. Wei, *Angew. Chem., Int. Ed.*, 2011, **50**, 2521–2525.
19 K. Micoine, B. Hasenknopf, S. Thorimbert, E. Lacôte and M. Malacria, *Org. Lett.*, 2007, **9**, 3981–3984.
20 M. P. Santoni, A. K. Pal, G. S. Hanan, M. C. Tang, K. Venne, A. Furtos, P. Menard-Tremblay, C. Malveau and B. Hasenknopf, *Chem. Commun.*, 2012, **48**, 200–202.
21 N. P. Luneva, S. A. Mironova, A. E. Shilov, M. Y. Antipin and Y. T. Struchkov, *Angew. Chem., Int. Ed. Engl.*, 1993, **32**, 1178–1179.
22 I. S. Tidmarsh, E. Scales, P. R. Prearley, J. Wolowska, L. Sorace, A. Caneschi, R. H. Laye and E. J. L. McInnes, *Inorg. Chem.*, 2007, **46**, 9743–9753.
23 D. C. Crans, F. Jiang, J. Chen, O. P. Anderson and M. M. Miller, *Inorg. Chem.*, 1997, **36**, 1038–1047.
24 F. Jiang, O. P. Anderson, S. M. Miller, J. Chen, M. Mahroof-Tahir and D. C. Crans, *Inorg. Chem.*, 1998, **37**, 5439–5451.
25 F. J. C. Rossotti and H. Rossotti, *Acta Chem. Scand.*, 1956, **10**, 957–984.
26 H. T. Evans, *Inorg. Chem.*, 1966, **5**, 967–977.
27 Q. Chen and J. Zubieta, *J. Chem. Soc., Chem. Commun.*, 1993, 1180–1182.
28 S. Khanra, L. J. Batchelor, M. Helliwell, F. Tuna, E. J. L. McInnes and R. E. P. Winpenny, *J. Mol. Struct.*, 2008, **890**, 157–162.
29 E. Scales, L. Sorace, A. Dei, A. Caneschi, C. A. Muryn, D. Collison and E. J. L. McInnes, *Chem. Sci.*, 2010, **1**, 221–225.
30 M. Hilbers, M. Meiwald and R. Mattes, *Z. Naturforsch., B: Chem. Sci.*, 1996, **51**, 57–67.
31 J. Spandl, I. Brüdgam and H. Hartl, *Angew. Chem., Int. Ed.*, 2001, **40**, 4018–4020.
32 J. Spandl, I. Brüdgam and H. Hartl, *Z. Anorg. Allg. Chem.*, 2003, **629**, 539–544.
33 D. D. Heinrich, K. Folting, W. E. Streib, J. C. Huffman and G. Christou, *J. Chem. Soc., Chem. Commun.*, 1989, 1411–1413.
34 J. R. Rambo, J. C. Huffman and G. Christou, *J. Am. Chem. Soc.*, 1989, **111**, 8027–8029.
35 S. L. Castro, Z. Sun, J. C. Bollinger, D. N. Hendrickson and G. Christou, *J. Chem. Soc., Chem. Commun.*, 1995, 2517–2518.
36 Z. Sun, C. M. Grant, S. L. Castro, D. N. Hendrickson and G. Christou, *Chem. Commun.*, 1998, 721–722.
37 S. L. Castro, Z. Sun, C. M. Grant, J. C. Bollinger, D. N. Hendrickson and G. Christou, *J. Am. Chem. Soc.*, 1998, **120**, 2365–2375.
38 H. Putz and K. Brandenburg, *Diamond*, Crystal Impact GbR, Bonn, Germany, 2014.
39 A. Müller, J. Döring, H. Bögge and E. Krickemeyer, *Chimia*, 1988, **42**, 300.
40 A. Müller, R. Sessoli, E. Krickemeyer, H. Bögge, J. Meyer, D. Gatteschi, L. Pardi, J. Westphal, K. Hovemeier, R. Rohlfing, J. Döring, F. Hellweg, C. Beugholt and M. Schmidtmann, *Inorg. Chem.*, 1997, **36**, 5239–5250.
41 P. Hermosilla-Ibáñez, W. Cañon-Mancisidor, J. Costamagna, A. Vega, V. Paredes-García, M. T. Garland, E. Le Fur, O. Cador, E. Spodine and D. Venegas-Yazigi, *Dalton Trans.*, 2014, **43**, 14132–14141.
42 J. T. Rijssenbeek, D. J. Rose, R. C. Haushalter and J. Zubieta, *Angew. Chem., Int. Ed. Engl.*, 1997, **36**, 1008–1010.
43 T. C. Stamatatos, K. A. Abboud, W. Wernsdorfer and G. Christou, *Angew. Chem., Int. Ed.*, 2007, **46**, 884–888.
44 H. Chen, Y. Zhang, Z.-B. Yu and J. Sun, *Dalton Trans.*, 2014, **43**, 15283–15286.
45 K. Kastner, J. T. Margraf, T. Clark and C. Streb, *Chem. – Eur. J.*, 2014, **20**, 12269–12273.

46 G. B. Karet, Z. Sun, D. D. Heinrich, J. K. McCusker, K. Folting, W. E. Streib, J. C. Huffman, D. N. Hendrickson and G. Christou, *Inorg. Chem.*, 1996, **35**, 6450–6460.
47 G. B. Karet, Z. Sun, W. E. Streib, J. C. Bollinger, D. N. Hendrickson and G. Christou, *Chem. Commun.*, 1999, 2249–2250.
48 K. Hegetschweiler, B. Morgenstern, J. Zubieta, P. J. Hagrman, N. Lima, R. Sessoli and F. Totti, *Angew. Chem., Int. Ed.*, 2004, **43**, 3436–3439.
49 C. P. Pradeep, D.-L. Long, G. N. Newton, Y.-F. Song and L. Cronin, *Angew. Chem., Int. Ed.*, 2008, **47**, 4388–4391.
50 P. Yin, A. Bayaguud, P. Cheng, F. Haso, L. Hu, J. Wang, D. Vezenov, R. E. Winans, J. Hao, T. Li, Y. Wei and T. Liu, *Chem. – Eur. J.*, 2014, **20**, 9589–9595.
51 A. Bayaguud, K. Chena and Y. Wie, *CrystEngComm*, 2016, **18**, 4042–4045.
52 P. Zabierowski, M. Radoń, J. Szklarzewicz and W. Nitek, *Inorg. Chem. Commun.*, 2014, **41**, 72–75.
53 G. Asgedom, A. Sreedhara, J. Kivikoski, J. Valkonen, E. Kolehmainen and C. P. Rao, *Inorg. Chem.*, 1996, **35**, 5674–5683.
54 D. F. Back, C. R. Kopp, G. M. de Oliveira and P. C. Piquini, *Polyhedron*, 2012, **3**, 21–29.
55 I. D. Brown and K. K. Wu, *Acta Crystallogr., Sect. B: Struct. Crystallogr. Cryst. Chem.*, 1976, **32**, 1957–1959.
56 W. Koenigs and G. Happe, *Ber. Dtsch. Chem. Ges.*, 1903, **36**, 2904–2910.
57 D. Menozzia, E. Biavardi, C. Massera, F.-P. Schmidtchen, A. Cornia and E. Dalcanal, *Supramol. Chem.*, 2010, **22**, 768–775.
58 P. Pana, M. Fujitaa, W.-Y. Ooia, K. Sudeshb, T. Takaradaa, A. Gotoc and M. Maeda, *Polymer*, 2011, **52**, 895–900.
59 Bruker AXS Inc., Madison, Wisconsin, USA, 1998.
60 G. M. Sheldrick, *Acta Crystallogr., Sect. A: Fundam. Crystallogr.*, 2008, **64**, 112–122.
61 A. L. Spek, *Acta Crystallogr., Sect. C: Cryst. Struct. Commun.*, 2015, **71**, 9–18.
62 A. L. Spek, *J. Appl. Crystallogr.*, 2003, **36**, 7–13.